

# Dalton Transactions

Accepted Manuscript



This is an *Accepted Manuscript*, which has been through the Royal Society of Chemistry peer review process and has been accepted for publication.

*Accepted Manuscripts* are published online shortly after acceptance, before technical editing, formatting and proof reading. Using this free service, authors can make their results available to the community, in citable form, before we publish the edited article. We will replace this *Accepted Manuscript* with the edited and formatted *Advance Article* as soon as it is available.

You can find more information about *Accepted Manuscripts* in the [Information for Authors](#).

Please note that technical editing may introduce minor changes to the text and/or graphics, which may alter content. The journal's standard [Terms & Conditions](#) and the [Ethical guidelines](#) still apply. In no event shall the Royal Society of Chemistry be held responsible for any errors or omissions in this *Accepted Manuscript* or any consequences arising from the use of any information it contains.

## A new simple Schiff base fluorescent “on” sensor for Al<sup>3+</sup> and its living cell imaging

Jutika Kumar, Manas Jyoti Sarma, Prodeep Phukan, Diganta Kumar Das\*

Department of Chemistry, Gauhati University, Guwahati, Assam, 781 014, INDIA. [digantakdas@gmail.com](mailto:digantakdas@gmail.com)

The simple Schiff base (Z)-N-benzylidenenaphthalen-1-amine (**L**) acts as an effective fluorescent sensor for Al<sup>3+</sup> by “off-on” mode and *ca.* 42 times enhancement in fluorescent intensity is observed. The detection limit of **L** towards Al<sup>3+</sup> is observed as 5×10<sup>-5</sup> M. UV/Visible and fluorescence data as well as DFT calculations confirms 1:3 coordination between Al<sup>3+</sup> and **L** through N atoms in a pyramidal shape. **L** is employed for imaging Al<sup>3+</sup> ion in living biological cells and for determination of Al<sup>3+</sup> ion in bovine serum albumin.

The simple Schiff base (Z)-N-benzylidenenaphthalen-1-amine is a fluorescent “on” sensor for  $Al^{3+}$ , applicable in biological cell and bovine serum albumin.

## Introduction

Aluminum (Al), the third most abundant metal in the earth's crust, is widely used in our daily life as electronic and electric components of different gadgets, building materials, different packaging items etc.  $\text{Al}^{3+}$  is a known neurotoxic to organisms<sup>1</sup> and is believed to cause Alzheimer's disease<sup>2</sup>.  $\text{Al}^{3+}$  interferes with the uptake of  $\text{Ca}^{2+}$  by plants and causes the retarded growth of plants<sup>3</sup>.  $\text{Al}^{3+}$  also restricts cell wall expansion leading to stunted roots<sup>4</sup> and contributes for oxidative damage of cell membrane<sup>5</sup>. Despite many drawbacks modern life can not avoid use of Al and hence there is big chance of  $\text{Al}^{3+}$  toxicity towards human health and environment. Hence designing new sensor for the detection of  $\text{Al}^{3+}$  has profound relevance.

Analytical methods based on atomic absorption and emission spectroscopy, spectrophotometry, electrochemistry, electrochemiluminescence etc. are known for  $\text{Al}^{3+}$  detection<sup>6-10</sup>. Operational simplicity, low detection limit, real-time detection and portability are the advantages of fluorescent metal ion sensors over other methods. Recently a number of fluorescent sensors for the determination of  $\text{Al}^{3+}$  have been reported. Fluorescent "off-on" sensor for  $\text{Al}^{3+}$  has been synthesized from 8-hydroxyquinoline-7-carbaldehyde and 4-aminopyrine which shows a 26 fold enhancement in intensity due to chelation enhanced fluorescence (CHEF)<sup>11</sup>. A quinoline-coumarine based fluorescent sensor of "off-on" type is recently reported<sup>12</sup>. Another fluorescent "off-on" type sensor reported which shows green fluorescence under UV radiation is based on perylene tetracarboxylic bisimide<sup>13</sup>. Schiff base receptor, 1-((E)-(1,3-dihydroxy-2-(hydroxymethyl)propan-2-ylimino)methyl) naphthalene-2-ol shows blue fluorescence enhancement for  $\text{Al}^{3+}$  in  $\text{CH}_3\text{OH}:\text{H}_2\text{O}$  medium<sup>14</sup>. 8-acetyl-7-hydroxy-4-methylcoumarin is reported to act as turn on fluorescent  $\text{Al}^{3+}$  sensor by emitting bright blue fluorescence under UV radiation<sup>15</sup>. A dual fluorescent turn "off" and colorimetric sensor

which shows a large red shift in fluorescent emission upon interaction with  $\text{Al}^{3+}$  is also reported<sup>16</sup>. A turn on fluorescent as well as colorimetric sensor based on 1-(2-pyridylazo)-2-naphthol is also known<sup>17</sup>. Most of these sensors for  $\text{Al}^{3+}$  are based on complicated synthetic procedures.

Simple Schiff's base ligands have been of recent interest as fluorescent sensor for metal ions including  $\text{Al}^{3+}$  due to their generally one step synthesis<sup>18-21</sup>. Thiazole based schiff base is recently reported as "off-on" fluorescent sensor for  $\text{Al}^{3+}$ <sup>22</sup>. A simple Schiff base based on o-nitrophenol has been reported as "off-on" type fluorescent sensor for  $\text{Al}^{3+}$  by *ca.* ten times enhancement in fluorescent intensity<sup>23</sup>. Another Schiff base sensor for  $\text{Al}^{3+}$  based on condensation of 8-hydroxyjulolidine-9-carboxaldehyde and benzhydrazide was reported by Lee et al<sup>24</sup>. Salicylimine, a condensation product of 2-hydroxyaniline and 2-hydroxybenzaldehyde, was also reported as fluorescent "on" sensor for  $\text{Al}^{3+}$  ion<sup>25</sup>. Condensation product of Salicylhydrazide and orthophthalaldehyde was reported as fluorescent probe for  $\text{Al}^{3+}$  in biological cells<sup>26</sup>. Schiff base derivative of salicylaldehyde and 4,4-Diuro-4-bora-3a,4a-diaza-sindacene (BDP) is also known as  $\text{Al}^{3+}$  sensor by emitting strong blue fluorescence<sup>27</sup>. Schiff base thiophene-2-carboxylic acid hydrazide has been reported as another  $\text{Al}^{3+}$  ion sensor through bright blue emission<sup>28</sup>. Aldehyde group was introduced into the 7 position of 8-hydroxyquinoline to form 8-hydroxyquinoline-7-carbaldehyde (HQ7A) which was condensed with 4-aminopyrine to obtain blue fluorescence emission  $\text{Al}^{3+}$  sensor<sup>29</sup>. Condensation product of 2-methyl quinoline-4-carboxylic hydrazide and 8-formyl-7-hydroxyl-4-methyl coumarin could also detect  $\text{Al}^{3+}$  by fluorescent "off-on" mode<sup>30</sup>. Another schiff base, perylenebisimide-based tetra salicylaldimine derivative, is known to detect  $\text{Al}^{3+}$  by emission of light green fluorescence<sup>31</sup>. Antipyridine based Schiff base is reported as turn on fluorescent sensor for  $\text{Al}^{3+}$ <sup>32</sup>. Reporting new fluorescent sensor of simple molecular structure for  $\text{Al}^{3+}$  is fascinating and of significance.

Herein, we report that the condensation product of 1-Naphthylamine and benzaldehyde, (Z)-N-benzylidenenaphthalen-1-amine (**L**), acts as fluorescent sensor for Al<sup>3+</sup> over a number of other metal ions by “off-on” mode. The sensor was successfully applied in fluorescent imaging of Al<sup>3+</sup> in living biological cells and bovine serum albumin.

## Experimental

Fluorescence spectra were recorded in Hitachi spectrophotometer. UV/Visible spectra were recorded in a Shimadzu UV 1800 spectrophotometer using 10 mm path length quartz cuvette. <sup>1</sup>H NMR spectra were recorded in a Bruker Ultrashield 300 MHz spectrometer. All <sup>1</sup>H NMR spectra were obtained in CDCl<sub>3</sub> at room temperature and the chemical shifts are reported in  $\delta$  values (ppm) relative to TMS. High resolution mass (HRMS) spectra were recorded in Agilent spectrometer using HPLC methanol as solvent. The measurements of pH were done in a digital pH meter (Merck).

All the chemicals and metal salts were purchased from Merck. Lead and silver salts are nitrates, mercury and calcium salts are chlorides while rest are sulphates. The metal salts were recrystallized from water (Millipore) before use. Solutions of **L** ( $5.0 \times 10^{-4}$  M) and metal salts ( $10^{-2}$  M) were prepared in 1:1 (v/v) CH<sub>3</sub>CN:H<sub>2</sub>O and H<sub>2</sub>O respectively.

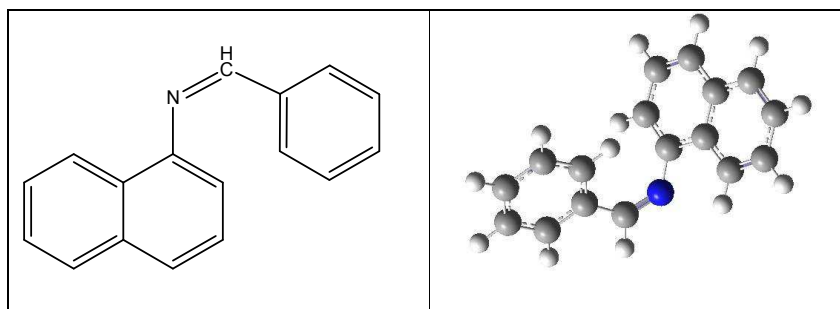
### Synthesis and characterisation of **L**

**L** has been synthesised by modification of reported procedure<sup>33</sup>, briefly: 1-Naphthylamine (0.136 g, 1.0 mmol) was dissolved in dichloromethane (20 mL). Benzaldehyde (0.106 g, 1.0 mmol) was added and the reaction mixture was refluxed for 10 hrs. After completion of reflux, the reaction mixture was diluted with dichloromethane and extracted successively with water and NaHCO<sub>3</sub> solution (10% aqueous). The organic extracts collected

were dried over anhydrous  $\text{Na}_2\text{SO}_4$  and the solvent was evaporated to obtain a liquid product of brown colour. Yield: 70%.

ESI-MS:  $[\text{M}+\text{H}]^+$ ,  $m/z$ , 232.11 ( $\text{C}_{17}\text{H}_{13}\text{N}$ , 100 % abundance); FT-IR: (KBr,  $\text{cm}^{-1}$ ): 1597.08 ( $\nu_{\text{C}=\text{N}}$ ), 3045 ( $\nu_{\text{C}-\text{H}}$ ), 1409 ( $\nu_{\text{C}=\text{C}}$ );  $^1\text{H}$ NMR: ( $\text{CDCl}_3$ ,  $\delta$  ppm, TMS): 8.57 (s, 1H); 8.38(m 1H); 8.06(m, 2H); 7.89(m, 1H); 7.76(d, 1H,  $J=8.4$ ); 7.57(m, 6H); 7.06(m, 1H);  $^{13}\text{C}$  NMR: ( $\text{CDCl}_3$ ,  $\delta$  ppm, TMS): 160.4, 149.2, 136.3, 133.8, 131.4, 128.9, 128.8, 128.5, 127.6, 126.3, 126.0, 123.9, 112.7.

## Results and discussion



Scheme 1: Chemical structure of **L** (left) and DFT optimised structure of **L** in Z form (right)

**L** ( $10^{-5}$  M) in 1:1 (v/v)  $\text{CH}_3\text{CN}:\text{H}_2\text{O}$  showed moderate fluorescence in the emission range 370 nm to 570 nm with  $\lambda_{\text{max}}$  at 430 nm when excited with 360 nm photons. Addition of  $\text{Al}^{3+}$  into the solution of **L** found to enhance the fluorescence intensity till the concentration of  $\text{Al}^{3+}$  became one third to that of **L** (Fig. 1). The fluorescence intensity did not increase on further addition of  $\text{Al}^{3+}$  with the final fluorescence intensity being *ca.* 42 times to that of the initial one.

Similar fluorescence titrations were carried out with metal ions –  $\text{Na}^+$ ,  $\text{K}^+$ ,  $\text{Ca}^{2+}$ ,  $\text{Mg}^{2+}$ ,  $\text{Mn}^{2+}$ ,  $\text{Fe}^{2+}$ ,  $\text{Fe}^{3+}$ ,  $\text{Co}^{2+}$ ,  $\text{Ni}^{2+}$ ,  $\text{Cu}^{2+}$ ,  $\text{Zn}^{2+}$ ,  $\text{Pb}^{2+}$ ,  $\text{Cd}^{2+}$ ,  $\text{Hg}^{2+}$ , and  $\text{Ag}^+$ . No significant change in fluorescence intensity of **L** was observed. In Fig. 2 we compare the effect of different metal ions along with  $\text{Al}^{3+}$  on the  $F/F_0$  values of **L** through

bar diagram.  $F$  and  $F_0$  are fluorescence intensities of **L** and **L** in presence of a metal ion respectively. It is clear from the figure that **L** could very well distinguish  $\text{Al}^{3+}$  over the rest of the metal ions.

The selectivity of **L** towards  $\text{Al}^{3+}$  in presence of another metal ion has also been established. For this purpose fluorescence intensity of **L** in presence of one equivalent of a metal ion ( $\text{Na}^+$ ,  $\text{K}^+$ ,  $\text{Ca}^{2+}$ ,  $\text{Mg}^{2+}$ ,  $\text{Mn}^{2+}$ ,  $\text{Fe}^{2+}$ ,  $\text{Fe}^{3+}$ ,  $\text{Co}^{2+}$ ,  $\text{Ni}^{2+}$ ,  $\text{Cu}^{2+}$ ,  $\text{Zn}^{2+}$ ,  $\text{Pb}^{2+}$ ,  $\text{Cd}^{2+}$ ,  $\text{Hg}^{2+}$  and  $\text{Ag}^+$ ) was recorded. One third equivalent of  $\text{Al}^{3+}$  was then added to the solution already containing the metal ion and fluorescence intensity was observed. The fluorescence intensity enhanced and the  $F/F_0$  ratio was found to be almost equivalent to that of **L** and  $\text{Al}^{3+}$  interaction containing no other metal ion (Fig. 3). However in case of  $\text{Cu}^{2+}$  the  $F/F_0$  value was found to be lower. This confirms that **L** has stronger affinity and hence selectivity for  $\text{Al}^{3+}$  in presence of metal ions -  $\text{Na}^+$ ,  $\text{K}^+$ ,  $\text{Ca}^{2+}$ ,  $\text{Mg}^{2+}$ ,  $\text{Mn}^{2+}$ ,  $\text{Fe}^{2+}$ ,  $\text{Fe}^{3+}$ ,  $\text{Co}^{2+}$ ,  $\text{Ni}^{2+}$ ,  $\text{Cu}^{2+}$ ,  $\text{Zn}^{2+}$ ,  $\text{Pb}^{2+}$ ,  $\text{Cd}^{2+}$ ,  $\text{Hg}^{2+}$ , and  $\text{Ag}^+$  except  $\text{Cu}^{2+}$ .

The interaction between **L** and  $\text{Al}^{3+}$  was also confirmed by UV-Visible spectroscopy (Fig. 4). Absorption maximum for **L** in 1:1 (v/v)  $\text{CH}_3\text{CN}:\text{H}_2\text{O}$  were observed at  $\lambda_{\text{max}}$  350 nm, 298 nm and 256 nm (sh). Gradual addition of  $\text{Al}^{3+}$  into the solution shifted the 350 nm peak to 338 nm, the 298 nm peak became a shoulder at 305 nm and the shoulder at 256 nm became a peak at 305 nm.

The binding constant of **L** with  $\text{Al}^{3+}$  has been determined using the modified Benesi–Hildebrand equation as shown below by the fluorescence method:

$$1/\Delta F = \Delta F_{\text{max}} + (1/K[\text{C}]^n) \times (1/\Delta F_{\text{max}})$$

where  $\Delta F = (F_x - F_0)$  and  $\Delta F_{\text{max}} = F_{\infty} - F_0$ , where  $F_0$ ,  $F_x$ , and  $F_{\infty}$  are the emission intensities of **L** in the absence of  $\text{Al}^{3+}$ , at an intermediate  $\text{Al}^{3+}$  concentration, and at a concentration of the complete interaction between **L** and  $\text{Al}^{3+}$ , respectively.  $K$  is the binding constant,  $C$  is the concentration of  $\text{Al}^{3+}$  and  $n$  is the number of  $\text{Al}^{3+}$  ions bound to each **L**. A linear plot was obtained for  $n =$

0.33 indicating association of three **L** per  $\text{Al}^{3+}$  (Fig. 5). The binding constant was calculated to be  $0.4 \times 10^6$ .

The effect of pH on the fluorescence intensity of **L** in the absence and presence of  $\text{Al}^{3+}$  was carried out in 100 mM HEPES buffer (Fig. 6). In case of **L** the plot of fluorescence versus pH showed a hump in the pH range 5.0 to 7.0 with maximum at pH 6.0. Beyond pH 7.0 the fluorescence intensity remained unchanged till pH 12.0. In case of  $\text{Al}:\text{3L}$  the fluorescence hump was not observed. The fluorescence intensity was found to decrease gradually till pH 7.2 and remained same thereafter till pH 11.2. Further increase in pH resulted in a decrease in fluorescence intensity till pH 12.0. At pH above 11.2  $\text{Al}^{3+}:\text{L}$  complex breaks down and  $\text{Al}(\text{OH})_3$  formed, **L** becomes free and hence fluorescence quenches due to PET.

The reversibility of **L** towards  $\text{Al}^{3+}$  ion was checked using different anions and disodium salt of ethylenediamine tetraacetate ( $\text{Na}_2\text{EDTA}$ ). The fluorescence intensity of  $\text{Al}:\text{3L}$  complex was found to quench upon addition of more than three equivalent of  $\text{NaNO}_3$ . This fluorescence quenched solution regains its fluorescence when  $\text{Al}_2(\text{SO}_4)_3$  was added. Interestingly addition of  $\text{Na}_2\text{EDTA}$  has no effect on the fluorescence intensity of  $\text{Al}:\text{3L}$  complex.

The fluorescent “off-on” behaviour may be explained on the basis of photoinduced electron transfer (PET) mechanism. In **L** the PET occurs from the electron density at N to the naphthylamine ring. Binding of  $\text{Al}^{3+}$  to **L** snaps this PET process leading to fluorescence enhancement. Further the DFT calculation has shown that  $\text{Al}^{3+}$  ion binding leads to the extension of  $\pi$  electron cloud of benzyl group up to N atom. This causes enhanced electron delocalisation in **L** which helps further enhancement in fluorescence intensity.

In order to substantiate the PET mechanism and hence involvement of N lone pair electron density for bond formation with  $\text{Al}^{3+}$  we recorded in solution FT-IR of  $\text{Al}^{3+}:\text{3L}$  complex. Before recording the FT-IR spectrum the completeness of complex

formation was checked by recording the fluorescence spectra which showed 42 times increase in fluorescence intensity. The observed significant change in the FT-IR spectrum recorded was that the  $1597\text{ cm}^{-1}$  peak of **L** due to  $\nu_{\text{C=N}}$  shifted to  $1629\text{ cm}^{-1}$ . DFT calculation showed that  $\text{Al}^{3+}$  interaction with **L** through N atom caused extension of benzyl electron density to C=N which resulted in higher wave number of  $\nu_{\text{C=N}}$  stretching. HRMS spectrum of  $\text{Al}^{3+}:\text{3L}$  complex was also recorded (complex formation was confirmed as for FT-IR) and molecular ion peak was observed at 722.4 which confirms the formation of the complex. To further confirm the interaction between **L** and  $\text{Al}^{3+}$ ,  $^1\text{H}$ NMR was recorded for **L** in presence of one third equivalent of  $\text{Al}^{3+}$ . A qualitative change in the  $^1\text{H}$ NMR spectrum was observed with the triplet at 8.38 – 8.35 ppm, quartet at 8.06 – 8.03 ppm and quartet at 7.89 – 7.86 becoming doublets without any significant change in peak positions. The multiplet observed for **L** in 7.50 – 7.4 ppm was found to shift to 7.09 – 7.08 ppm as a quartet. Fig. 7 compares the  $^1\text{H}$ NMR of **L** and  $\text{Al}^{3+}:\text{3L}$ .

### DFT Calculation

The structure of **L** and its  $\text{Al}^{3+}$  complex were fully optimized using B3LYP<sup>34</sup> function. For **L** the basis set 6-311G++ was used and for the  $\text{Al}^{3+}$  complex of **L** the basis set LanL2DZ was used in the program Gaussian 09<sup>35</sup>. To confirm the stability of the complex the vibrational energy calculation was also performed with same level of theory. **L** was optimised for both E and Z conformations and were found to be of similar stability. The energies of E and Z conformation were found to be -710.380 a.u. and -710.370 a.u. respectively. The complex formation between **L**, both E and Z forms, and  $\text{Al}^{3+}$  were studied by DFT and it was observed that only Z form of **L** takes part in complex formation. Three **L** were found to bind  $\text{Al}^{3+}$  through its N atoms forming a three coordinate complex (Fig. 8). The three N atoms are not planar but forms a pyramidal geometry together with  $\text{Al}^{3+}$ . Fig. 9 shows the shapes of

HOMO and LUMO for **L** and  $\text{Al}^{3+}$ :3**L** complex. From the optimized structure of  $\text{Al}^{3+}$ :3**L** complex it was observed that the  $\pi$  electron cloud of benzyl group was extended up to nitrogen atom. Again from DFT optimized HOMO-LUMO orbital it was seen that in the complex only **L** contributes to the HOMO, on the other hand  $\text{Al}^{3+}$  and **L** both contribute to LUMO.

### Living biological cell studies

Finally, we studied the bioimaging application of **L** for sensing  $\text{Al}^{3+}$  in living human embryonic kidney (HEK) cell. 10  $\mu\text{L}$  of **L** (5  $\mu\text{M}$ ) was incubated with 990  $\mu\text{L}$  of cell solution in Dobacco modified eagle medium (DMEM) for 3 hour at 25  $^{\circ}\text{C}$ . Just before completion of incubation 10  $\mu\text{L}$   $\text{Al}^{3+}$  solution (5  $\mu\text{M}$  in DMEM) was added and incubated for further 3 hour at 25  $^{\circ}\text{C}$ . At the completion of incubation the excess  $\text{Al}^{3+}$  were removed by washing with phosphate buffer saline (PBS) solution. Fluorescence microscope images were recorded for cell solution, **L** + cell solution and **L** + cell +  $\text{Al}^{3+}$  solution (Fig. 10). The bright circular shapes in Fig. 9C are the regions of higher  $\text{Al}^{3+}$  concentration. From the figure it is clear that **L** could nicely recognise  $\text{Al}^{3+}$  in living cells.

### Application in $\text{Al}^{3+}$ determination in bovine serum albumin

The sensor **L** was successfully applied in the determination of  $\text{Al}^{3+}$  in aqueous solution of bovine serum albumin (BSA). Fig 11A shows the fluorescence intensity enhancement for **L** in BSA medium. Fig. 11B is the plot of fluorescence intensity as a function of  $\text{Al}^{3+}$  concentration. An enhancement in fluorescence intensity of *ca.* 30 times has been observed.

### Reversibility of **L** towards $\text{Al}^{3+}$

The reversibility of **L**  $\text{Al}^{3+}$  was checked by employing different anions and  $\text{Na}_2\text{EDTA}$ .  $\text{NaNO}_3$  was found to start quench the

fluorescence intensity of  $\text{Al}^{3+}:\text{3L}$  complex when its added concentration became higher than one equivalent to  $\text{Al}^{3+}:\text{3L}$  complex. The fluorescence quenches almost completely when added  $\text{NaNO}_3$  became three equivalent to  $\text{Al}^{3+}:\text{3L}$  complex. We did not observe any fluorescence quenching when  $\text{Na}_2\text{EDTA}$  was added to  $\text{Al}^{3+}:\text{3L}$  complex solution.

### Acknowledgement

The DST, New Delhi and UGC, New Delhi are thanked for financial assistance to the Department through FIST and SAP respectively. IIT-Guwahati is thanked for biological cell imaging studies (Department of Biotechnology) and HRMS (SAIF).

## Notes and references

- 1 R. A. Yokel, *Fundam. Appl. Toxicol.*, 1987, **9**, 795; G. Muller, V. Bernuzzi and D. Desor, *Teratology*, 1990, **42**, 253; J. M. Donald and M. S. Golub, *Neurotoxicol. Teratol.*, 1989, **11**, 341.
- 2 D. R. Crapper, S. S. Krishnan and A. J. Dalton, *Science*, 1973, **180**, 511; D. P. Perl and A. R. Brody, *Science*, 1980, **208**, 297; E. House, J. Collingwood, A. Khan, O. Korchazkina, G. Berthon and C. J. Exley, *J. Alzheimers Dis.*, 2004, **6**, 291.
- 3 R. W. Gensemer and R. C. Playle, *Crit. Rev. Environ. Sci. Technol.*, 1999, **29**, 315.
- 4 C. Meriño-Gergichevich, M. Alberdi, A. G. Ivanov and M. Reyes-Díaz, *J. Plant Nutr. Soil Sci.*, 2010, **10**, 217.
- 5 A. Budimir, *Acta Pharmaceutica*, 2011, **61**, 1; P. Nayak, *Environ. Research A*, 2002, **89**, 101; P. Zatta, *Coord. Chem. Reviews*, 2002, **228**, 271.
- 6 H. Sang, P. Liang and D. Du, *J. Hazard. Materials*, 2008, **154**, 1127.
- 7 S.J. Djane, M. Gra and C. Korn, *Spectrochim. Acta Part B: Molecular and Biomolecular spectroscopy*, 2000, **55**, 389.
- 8 S. Abbasi and A. Farmany, *Food Chem.*, 2009, **116**, 1019.
- 9 D. Brian, M.S. Brooks and M.M. Richter, *Anal. Chem.* 2003, **75**, 1102.
- 10 V.K. Gupta, A.K. Jain and G. Maheshwari, *Talanta*, 2007, **72**, 1469.
- 11 L. Fan, Xin-hui Jiang, Bao-dui Wang and Zheng-yin Yang, *Sens. and Actuat. B*, 2014, **205**, 249.
- 12 Jing-can Qin, Tian-rong Li, Bao-dui Wang, Zheng-yin Yang and L. Fan, *Spectrochim. Acta Part A: Molecular and Biomolecular Spectroscopy*, 2014, **133**, 38.
- 13 S. Malkondu, *Tetrahedron*, 2014, **70**, 5580.
- 14 D.H. Kima, Y.S. Im, H. Kimb and C. Kima, *Inorg. Chem. Com.*, 2014, **45**, 15.

- 15 T. Li, R. Fang, B. Wang, Y. Shao, J. Liu, S. Zhang and Z. Yang, *Dalton Trans.* 2014, **43**, 2741.
- 16 R. Patil, A. Moirangthem, R. Butcher, N. Singh, A. Basu, K. Tayade, U. Fegade, D. Hundiware and A. Kuwar, *Dalton Trans.*, 2014, **43**, 2895.
- 17 V. K. Gupta, S. K. Shoorra, L. K. Kumawat, A. K. Jain, *Sens. Actuators B* 2015, **209**, 15.
- 18 K. Dutta, R. C. Deka and D. K. Das, *Spectrochim. Acta A*, 2014, **124**, 124-129.
- 19 K. Dutta, R. C. Deka and D. K. Das, *J Luminescence*, 2014, **148** 325-329.
- 20 D. K. Das, P. Goswami and B. Medhi, *J Fluorescence*, 2014, **145**, 454-458.
- 21 J. Kumar, P. Bhattacharyya, D. K. Das, *Spectrochim Acta Part A: Molecular and Biomolecular Spectroscopy*, 2014, 2015, **138**, 99.
- 22 V. K. Gupta, A. K. Singh, L. K. Kumawat, *Sens. Actuators B* 2014, **195**, 98)
- 23 C.H. Chen, D.J. Liao, C.F. Wan and A.T. Wu, *Analyst*, 2013, **138**, 2527).
- 24 S.A. Lee, G. R. You, Y.W. Choi, H.Y. Jo, A.R. Kim, I. Noh, S.J. Kim, Y. Kim and C. Kim, *Dalton Trans.*, 2014, **43**, 6650.
- 25 S. Kim, J.Y. Noh, K.Y. Kim, J.H. Kim, H.K. Kang, S.W. Nam, S.H. Kim, S. Park, C. Kim and J. Kim, *Inorg. Chem.* 2012, **51**, 3597.
- 26 L. Wang, W. Qin, X. Tang, W. Dou, W. Liu, Q. Teng and X. Yao, *Org. Biomol. Chem.*, 2010, **8**, 3751.
- 27 R. Kang, X. Shao, F. Peng, Y. Zhang, G.T. Sun, W. Zhao and X.D. Jiang, *RSC Adv.*, 2013, **3**, 21033).
- 28 K. Tiwari, M. Mishra and V.P. Singh, *RSC Adv.*, 2013, **3**, 12124)
- 29 L. Fan, X. Jiang, B. Wang, Z. Yang, *Sens. Actuat. B*, 2014, **205**, 249)

- 30 J. Qin, T. Li, B. Wang, Z. Yang, L. Fan, *Spectrochim. Acta Part A: Molecular and Biomolecular Spectroscopy*, 2014, **133**, 38.
- 31 S. Malkondu, *Tetrahedron* 2014, **70**, 5580.
- 32 V. K. Gupta, A. K. Singh, N. Mergu, *Electrochim. Acta* 2014, **117**, 405–412.
- 33 Y.S. Lan, B.S. Liao, Y.H. Liu, S.M. Peng and S.T. Liu, *Euro. J. Org. Chem.* 2013, **23**, 5160.
- 34 A. D. Becke, *J. Chem. Phys.* 1993, **98**, 5648–5652; C. Lee, W. Yang, R.G. Parr, *Phys. Rev. B*, 1988, **37**, 785–789.
- 35 M.J. Frisch, G.W. Trucks, H.B. Schlegel, G.E. Scuseria, M.A. Robb, J.R. Cheeseman, G. Scalmani, V. Barone, B. Mennucci, G.A. Petersson, H. Nakatsuji, M. Caricato, X. Li, H.P. Hratchian, A.F. Izmaylov, J. Bloino, G. Zheng, J.L. Sonnenberg, M. Hada, M. Ehara, K. Toyota, R. Fukuda, J. Hasegawa, M. Ishida, T. Nakajima, Y. Honda, O. Kitao, H. Nakai, T. Vreven, J. A. Montgomery, Jr., J.E. Peralta, F. Ogliaro, M. Bearpark, J.J. Heyd, E. Brothers, K.N. Kudin, V.N. Staroverov, T. Keith, R. Kobayashi, J. Normand, K. Raghavachari, A. Rendell, J.C. Burant, S.S. Iyengar, J. Tomasi, M. Cossi, N. Rega, J. M. Millam, M. Klene, J.E. Knox, J.B. Cross, V. Bakken, C. Adamo, J. Jaramillo, R. Gomperts, R.E. Stratmann, O. Yazyev, A. J. Austin, R. Cammi, C. Pomelli, J.W. Ochterski, R.L. Martin, K. Morokuma, V.G. Zakrzewski, G.A. Voth, P. Salvador, J.J. Dannenberg, S. Dapprich, A.D. Daniels, O. Farkas, J.B. Foresman, J.V. Ortiz, J. Cioslowski and D.J. Fox, Gaussian, Inc., Wallingf, Gaussian 09, Revision B.01.

Fig. 1: Effect of  $\text{Al}^{3+}$  on the fluorescence emission spectra of **L** in 1:1 (v/v)  $\text{CH}_3\text{CN}:\text{H}_2\text{O}$ .

Fig. 2:  $F/F_0$  response of **L** towards different metal ions in 1:1 (v/v)  $\text{CH}_3\text{CN}:\text{H}_2\text{O}$ . Here,  $F_0$  and  $F$  are fluorescence intensity of **L** in absence of metal ion and in presence of 1/3 equivalent of the metal ion.

Fig. 3:  $F/F_0$  response of **L** in presence of (i)  $\text{Al}^{3+}$  (black bars); (ii)  $\text{Al}^{3+}$  and another metal ion (gray bars) in 1:1 (v/v)  $\text{CH}_3\text{CN}:\text{H}_2\text{O}$ . Similar heights of black and grey bars confirm selectivity of **L** towards  $\text{Al}^{3+}$  over other metal ions (exception  $\text{Cu}^{2+}$ ).

Fig. 4: Change in UV/Visible spectra of **L** in 1:1 (v/v)  $\text{CH}_3\text{CN}:\text{H}_2\text{O}$  at different added concentration of  $\text{Al}^{3+}$ .

Fig. 5: The plot of  $1/\Delta F$  versus  $[\text{Al}^{3+}]^n$  for  $n=1$  ( $\blacktriangle$ ) and  $0.33$  ( $\blacksquare$ ) to confirm the number of **L** binding to one  $\text{Al}^{3+}$  using Benesi-Hildebrand equation. The higher linearity of the plot for  $n=0.33$  confirms that three **L** binds one  $\text{Al}^{3+}$ .

Fig. 6: Effect of pH on the fluorescent intensity of **L** ( $\bullet$ ) and  $\text{Al}^{3+}:\text{3L}$  ( $\blacksquare$ ) in 1:1 (v/v)  $\text{CH}_3\text{CN}:\text{H}_2\text{O}$ .

Fig. 7:  $^1\text{H}$ NMR of **L** and **L** in presence of one third equivalent of  $\text{Al}^{3+}$ . The peak positions where change occurred has been encircled.

Fig. 8: DFT optimised structure of  $\text{Al}^{3+}\text{L}_3$  complex to show that the Z form of **L** is taking part in complex formation (A) and the three N atoms (blue balls) coordinate to  $\text{Al}^{3+}$  (pink ball) in pyramidal fashion (B).

Fig. 9: HOMO and LUMO of **L** and  $\text{Al}^{3+}\text{L}_3$ .

Fig. 10: Fluorescence image of HEK cell solution (A), HEK cell in presence of  $\text{Al}^{3+}$  ions (B), HEK cell in presence of **L** and  $\text{Al}^{3+}$  (C).

Fig. 11: In aqueous bovine serum albumin medium - Fluorescence spectra of **L** (A) and plot of fluorescence intensity versus  $\text{Al}^{3+}$  concentration (B).

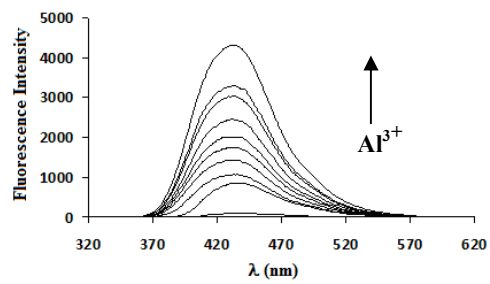


Fig. 1

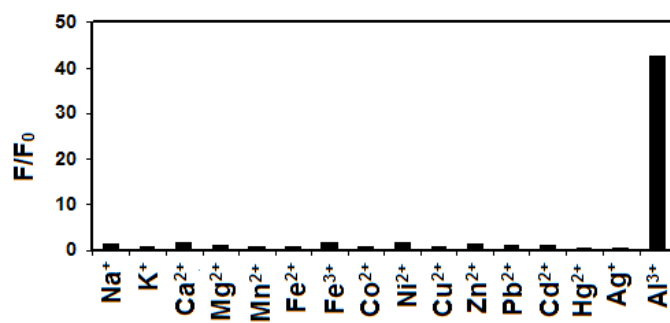


Fig. 2

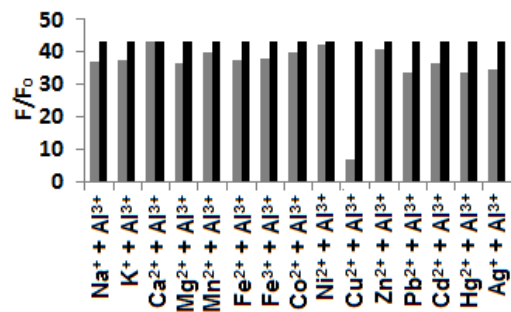


Fig. 3:

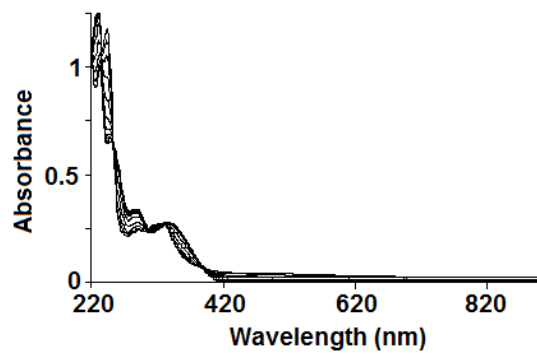


Fig. 4

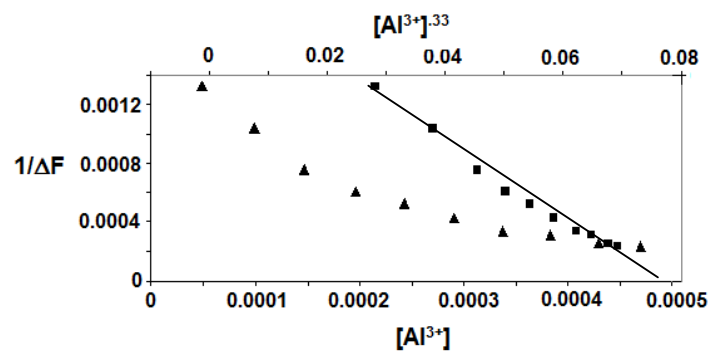


Fig. 5

Fig. 5:

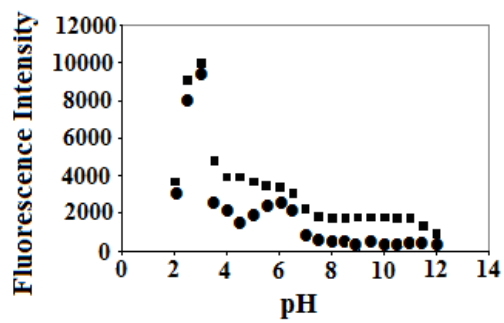


Fig. 6

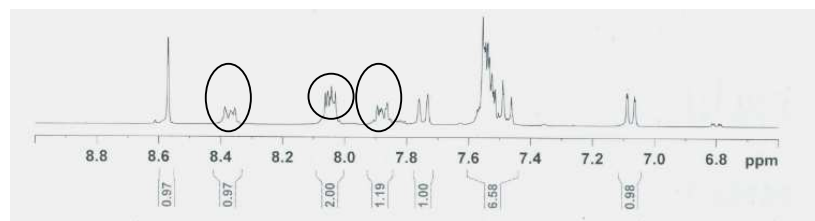
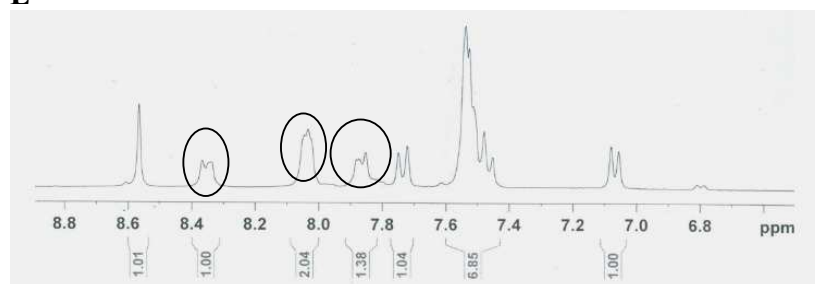
**L****L + 0.33 Al<sup>3+</sup>**

Fig. 7

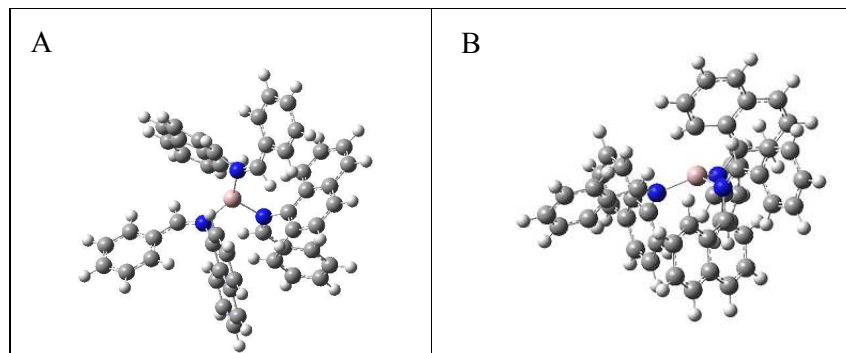


Fig. 8

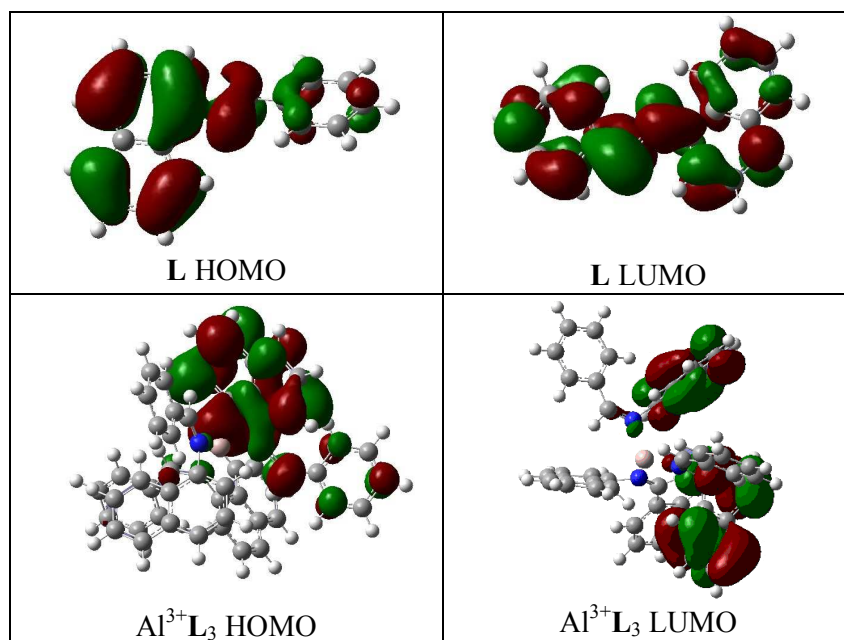


Fig. 9

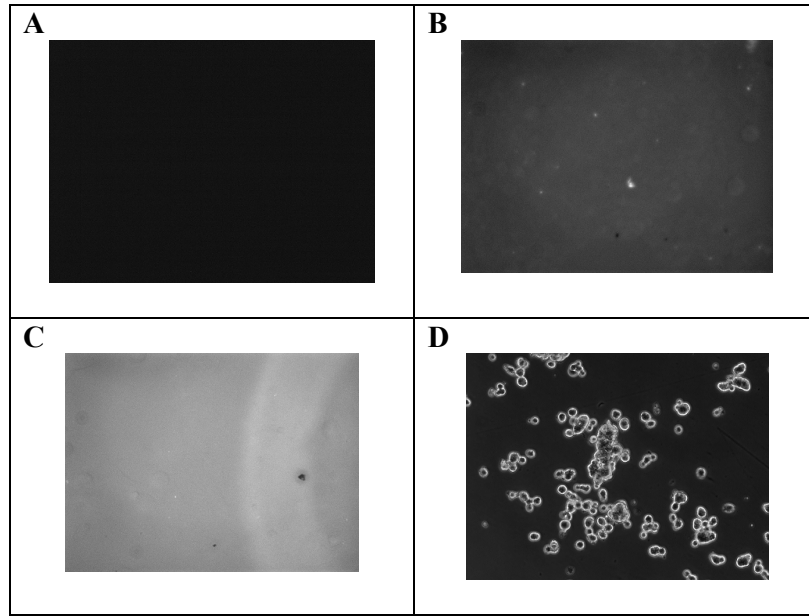


Fig. 10

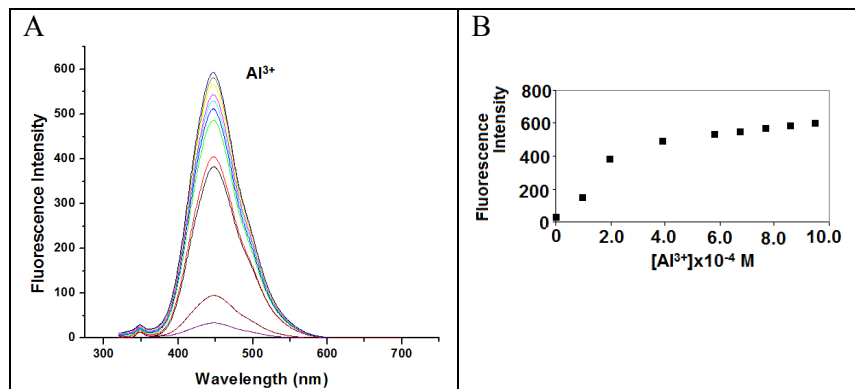
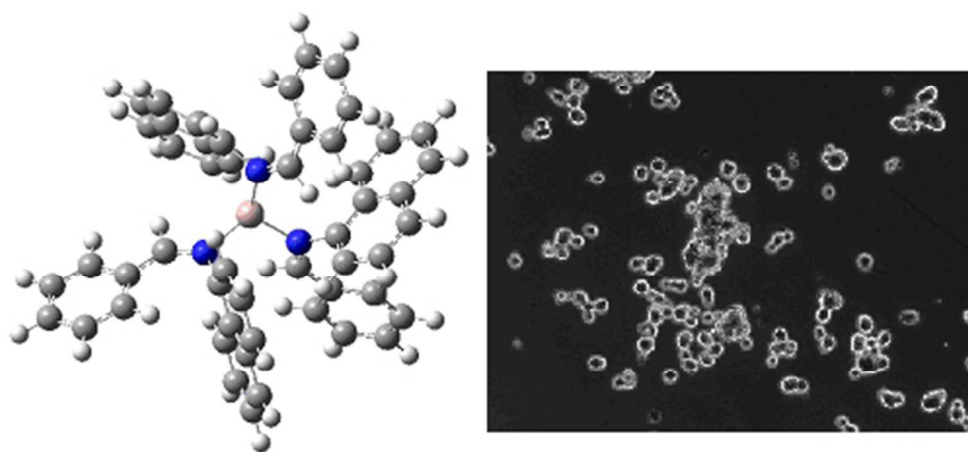


Fig. 11



135x64mm (96 x 96 DPI)